

constant for neutron-neutron, neutron-proton, and proton-proton systems, the value for  $a_{np} = -22.5$  F implies that the multipion pole strength  $\Gamma_{nn}$  departs from the exact charge symmetry by  $\sim 2-2.5\%$ .

#### ACKNOWLEDGMENTS

The authors would like to express their deep gratitude to Dr. A. I. Baz, Dr. C. Fronsdal, and Dr. R. P. Haddock for stimulating discussions.

They are indebted to Dr. D. L. Lin and Dr. Lj. Novaković for sending them their results prior to publication. The authors' deep appreciation belongs to D. Miler, who did the statistical analysis of the theoretical fit to the experimental data.

The skillful operation of the neutron generator team is appreciated. The authors are grateful to the members of the electronic division for the maintenance of the apparatus.

## Deuteron Stripping Studies in the Light Isotopes of Nickel\*

R. H. FULMER, A. L. MCCARTHY, AND B. L. COHEN  
*University of Pittsburgh, Pittsburgh, Pennsylvania*

AND

R. MIDDLETON†  
*Atomic Weapons Research Establishment, Aldermaston, Berkshire, England*  
(Received 7 October 1963)

Measurements of protons from  $(d,p)$  reactions on  $\text{Ni}^{58}$  and  $\text{Ni}^{60}$  were made with the Aldermaston tandem Van de Graaff and multigap spectrograph. A large number of states of the final nuclei (well over a hundred in each case) were observed and assigned to single-particle states. For the states in the  $28 < N \leq 50$  shell, the results for both energies and degree of filling are compared with pairing theory; the agreement is good. A sufficiently large fraction of the  $l=2$  states are observed to locate the  $d_{5/2}$  and  $d_{3/2}$  single-particle states at 6.0 and 9.3 MeV, respectively, in  $\text{Ni}^{58}$ , and at 5.0 and 8.4 MeV, respectively, in  $\text{Ni}^{61}$ . A relation between neutron-reduced width  $\Gamma_n^0$  (from neutron experiments) and the stripping spectroscopic factor  $S$  is derived and checked experimentally with two levels observed in both experiments; the agreement is satisfactory. Plots of neutron strength function versus energy are obtained containing both neutron and stripping data, and subjected to the requirements of  $\Sigma S=1$  and width  $=2W$  (where  $W$  is the depth of the imaginary potential in optical model). The results give the location of the  $3s_{1/2}$  states as 7.3 MeV in  $\text{Ni}^{59}$  and 6.0 MeV in  $\text{Ni}^{61}$ . The distribution of states belonging to each single-particle state is found to have approximately the expected width  $2W$  except for the  $g_{9/2}$  state in  $\text{Ni}^{61}$  which is concentrated in a single nuclear level. It is shown that the latter behavior is expected since there are no other positive-parity states expected even nearly within a distance  $W$  of the single-particle state. In  $\text{Ni}^{59}$ , the situation is similar except that states are expected and found at a distance  $\approx 1.5W$ , and these are mixed in weakly.

### I. INTRODUCTION

THE reactions  $\text{Ni}^{58}(d,p)\text{Ni}^{59}$  and  $\text{Ni}^{60}(d,p)\text{Ni}^{61}$  have been studied by the present authors<sup>1</sup> and by other investigators.<sup>2-5</sup> In our previous study,<sup>1</sup> we located the single-particle states of  $\text{Ni}^{59}$  and  $\text{Ni}^{61}$ ; these states were taken as the centers of gravity of the corre-

sponding nuclear levels. It is clear that all the principal nuclear levels of a given shell-model state must be observed and identified to give an accurate center of gravity. In Ref. 1 we gave evidence that not all the  $3s_{1/2}$  levels were observed, because they occur in an energy region where the increasing level density made it difficult and finally impossible to resolve individual levels. The situation with the  $2d_{5/2}$  and  $2d_{3/2}$  states was even less satisfactory, for the same reason.

In this paper we present the results of a recent and more thorough investigation of the  $(d,p)$  reactions on  $\text{Ni}^{58}$  and  $\text{Ni}^{60}$ , with resolution better by a factor of two than that of Ref. 1. The high resolution spectra were obtained with the Aldermaston tandem Van de Graaff accelerator. The data yielded new information principally in the energy region of  $s$  and  $d$  levels. Revised centers of gravity of the  $s_{1/2}$ ,  $d_{5/2}$ , and  $d_{3/2}$  states, and also of the  $p_{3/2}$ ,  $p_{1/2}$ , and  $f_{5/2}$  states are given on the

\* Supported in part by the National Science Foundation and the U. S. Office of Naval Research.

† Present address: University of Pennsylvania, Philadelphia, Pennsylvania.

<sup>1</sup> B. L. Cohen, R. H. Fulmer, and A. L. McCarthy, *Phys. Rev.* **126**, 698 (1962).

<sup>2</sup> J. P. Schiffer, L. L. Lee, Jr., and B. Zeidman, *Phys. Rev.* **115**, 427 (1959).

<sup>3</sup> C. H. Paris, Massachusetts Institute of Technology Laboratory for Nuclear Science Progress Report, 1 May 1959 (unpublished), p. 116.

<sup>4</sup> H. A. Enge and R. A. Fisher, Massachusetts Institute of Technology Laboratory for Nuclear Science Progress Report, 1 May 1959 (unpublished), p. 124.

<sup>5</sup> A. W. Dalton, G. Parry, H. D. Scott, and S. Swierszczewski, *Proc. Phys. Soc. (London)* **77**, 682 (1961).

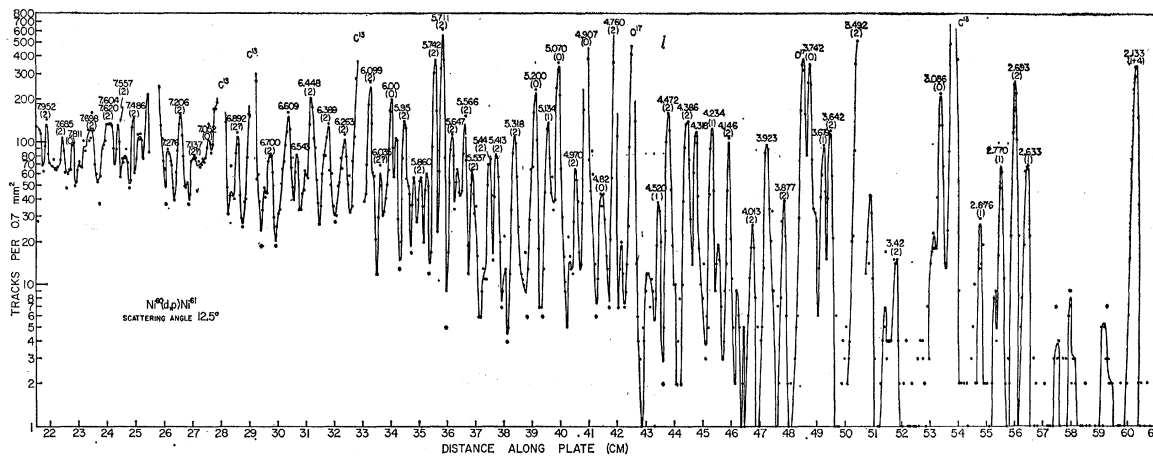


FIG. 1. Measured proton energy spectrum from  $\text{Ni}^{60}(d,p)\text{Ni}^{61}$ . Numbers above peaks are excitation energies in  $\text{Ni}^{61}$  in MeV, and  $l$  values assigned to these peaks are in parentheses. Energy resolution here is typical of the experiment.

basis of further identification of levels and new spin assignments.

## II. EXPERIMENTAL PROCEDURE

The basic experimental techniques have been described previously.<sup>6</sup> Specific details are as follows: The targets were isotopically enriched foils of  $\text{Ni}^{58}$  and  $\text{Ni}^{60}$  evaporated onto thin carbon backings to a thickness of about  $100 \mu\text{g}/\text{cm}^2$ . The targets were bombarded with 12-MeV deuterons from the Aldermaston tandem Van de Graaff accelerator, and the resulting protons were

analyzed by the multigap magnetic spectrograph which simultaneously recorded data on nuclear emulsions at angular intervals of  $7.5^\circ$ . A typical spectrum is shown in Fig. 1.

The major proton groups were identified and their energies assigned by comparison with the spectra of Ref. 1. The energies of the remaining proton groups were obtained by interpolation. For the proton groups at excitation energies higher than those measured in Ref. 1, the position of carbon impurity peaks of known  $Q$  value provided an extrapolation of the energy scale. The uncertainty in the measured excitation energy increases with excitation energy to a value of about 50 keV at 9 MeV.

The errors in the relative cross sections are estimated to be less than 15%. Absolute cross sections have not been determined because of the large ( $\sim 40\%$ ) uncertainty in target thicknesses.

The values of the angular momentum transfers were found by comparing the angular distributions of proton groups with distorted-wave Born-approximation (DWBA) calculations.<sup>7</sup> Representative angular distributions are shown in Fig. 2.

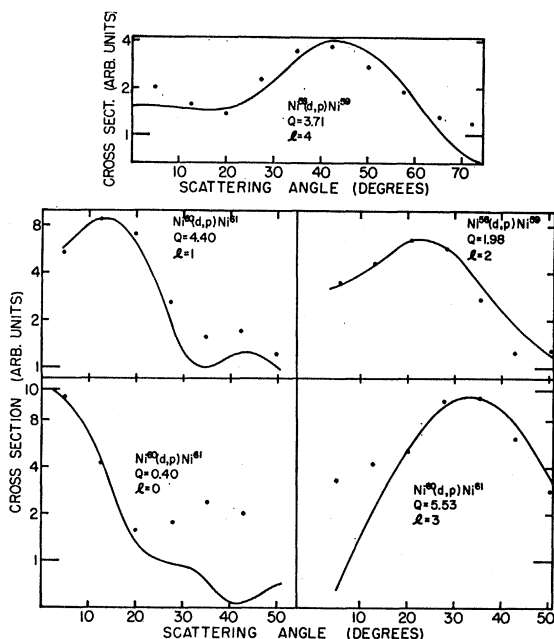


FIG. 2. Measured angular distributions for certain peaks from  $\text{Ni}(d,p)$  reactions and comparison with DWBA calculations. The solid lines are DWBA curves; the points are experimental values.

<sup>6</sup> R. Middleton and S. Hinds, Nucl. Phys. **34**, 404 (1962).

<sup>7</sup> G. R. Satchler, R. Bassel, and R. Drisko (private communication). The authors are greatly indebted to Dr. Satchler and his group for performing the DWBA calculations for the cases of interest here. They are based on the theory of Tobacman [Phys. Rev. **94**, 1655 (1954); Phys. Rev. **115**, 99 (1959)]. The real optical potential used is of the Saxon form; for the deuterons  $V=79.5$  MeV,  $r_0=1.274$  F, and  $a=0.739$  F; for the protons  $V=47$  MeV,  $r_0=1.25$  F, and  $a=0.65$  F. The imaginary optical potential is in the form of surface absorption; for the deuterons  $W=82$  MeV,  $r_0=1.389$  F, and  $a=0.625$  F; for the protons  $W=42$  MeV,  $r_0=1.25$  F, and  $a=0.47$  F. The cross sections from the output of the IBM calculations were multiplied by the factor 1.5 to account for finite range effects. Two lower cutoffs on radial integrations, 5.03 F and 5.62 F, gave negligible differences in cross section; the upper cutoff was large enough to include all contributions to the integral. The neutron binding energy was taken as  $Q+2.23$  MeV.

III. RESULTS

The experimental results for Ni<sup>59</sup> and Ni<sup>61</sup> are summarized in Tables I and II, respectively. The tables list, in successive columns, the energies of the observed nuclear levels and corresponding values of the angular momentum transfer *l*, the relative (*d, p*) cross section, and the spectroscopic factor *S*. This last factor is found by the relation

$$\frac{d\sigma}{d\omega} = \frac{(2J+1)}{(2I+1)} \sigma(l, \theta, Q) S, \quad (1)$$

in which *dσ/dω* is the experimental cross section, *J* the spin of the final state, and *I* the spin of the initial state in the stripping process. The quantity  $\sigma(l, \theta, Q)$  is calculated by DWBA methods<sup>7</sup>; it depends on the angular momentum transfer, the scattering angle  $\theta$ , and the *Q* value of the reaction.

The magnitudes of the relative spectroscopic factors determined from Eq. (1) have been put on an approximately absolute basis by normalizing the av *S* values for a large number of prominent levels to the results of Ref. 1; separate normalization factors were determined

TABLE I. Results of the Ni<sup>58</sup>(*d, p*)Ni<sup>59</sup> reactions.

This paper							Ref. 1						
(1) Excitation energy (MeV)	(2) <i>l</i>	(3) <i>(dσ/dω)<sub>max</sub></i> (Relative units)	(4) <i>(2J+1)S</i>	(5) <i>l</i>	(6) <i>(dσ/dω)<sub>max</sub></i> (mb/sr)	(7) <i>(2J+1)S</i>	(1) Excitation energy (MeV)	(2) <i>l</i>	(3) <i>(dσ/dω)<sub>max</sub></i> (Relative units)	(4) <i>(2J+1)S</i>	(5) <i>l</i>	(6) <i>(dσ/dω)<sub>max</sub></i> (mb/sr)	(7) <i>(2J+1)S</i>
0	1	~17 200	2.77	1	14.30	2.98	6.513	2	835	0.083			
0.340	3	2565	5.19	3	1.79	4.31	6.544	(2)	183	0.018			
0.471	1	8250	1.24	1	7.28	1.41	6.597	0	780	0.022			
0.887	1	2237	0.311	1	1.88	0.344	6.618	2	410	0.040			
1.318	1	4580	0.561	1	3.51	0.600	6.657	2	2800	0.270			
1.348	...	57	...				6.716	2	2080	0.198	2	2.39	0.368
1.696	(3)	394	0.605	(3)	0.313	0.580	6.741	2	1925	0.182	2	3.00	0.448
1.748	(1)	275	0.031				6.843	2	770	0.072			
1.967	...	~100	...				6.931	0	1950	0.064			
2.422	(1)	257	0.025	4	0.102	0.383	6.967	0	~2140	~0.07	0	1.33	0.043
2.640	3	245	0.307	3	0.302	0.043	7.021	2	1775	0.159	0	1.95	0.059
2.698	...	228	...		0.240	0.358	7.080	2	500	0.047	(0)	1.53	0.046
2.910	1	71.5	0.006				7.129	2	641	0.056			
3.045	1	364	0.032				7.170	...	505	...			
3.071	4	2690	7.50	4	2.52	7.90	7.199	...	~1200	...	2	2.32	0.332
3.151	...	84.5	...				7.245	2	1090	0.093			
3.203	1	348	0.030	1	0.364	0.045	7.287	2	1060	0.090			
3.384	2	55	0.011				7.362	2	972	0.076			
3.421	0	2760	0.046	(0)	1.08	0.060	7.394	2	722	0.060			
3.468	1	1870	0.154	1	1.30	0.153	7.417	2	1257	0.103			
3.559	2	1074	0.197	2	0.871	0.218	7.448	2	1970	0.155	2	2.40	0.325
3.661	2	126	0.031				7.540	0	1230	0.055			
3.711	2	96	0.017				7.566	...	~1400	...			
3.748	...	128	...	3	0.062	0.081	7.601	2	1750	0.139	(2)	2.78	0.371
3.874	1	1314	0.101	1	1.12	0.124	7.618	2	910	0.071			
3.920	...	49	...				7.643	2	1632	0.128			
4.031	1	696	0.052	1	0.600	0.065	7.700	(0)	1870	0.091			
4.054	(0)	96	0.002				7.737	...	1087	...			
4.145	1	740	0.054	1	0.702	0.078	7.809	(2)	1630	0.124	0	1.20	0.034
4.210	2	395	0.064				7.875	...	~1500	...			
4.256	(1)	1660	0.118	1	1.68	0.178	7.910	(2)	1495	0.111			
4.294	...	160	...				7.938	...	495	...			
4.469	4	181	0.408				7.972	2	1820	0.139			
4.505	2	9500	1.44	2	7.60	1.64	8.019	2	1425	0.103			
4.611	2	97	0.014				8.055	2	2090	0.155			
4.652	...	72	...				8.183	2	947	0.067			
4.691	4	328	0.716				8.216	2	786	0.055			
4.734	1	1210	0.078	1	1.42	0.139	8.240	2	737	0.050			
4.808	2	1800	0.257	2	1.42	0.289	8.269	2	740	0.051			
4.883	1	69.5	0.005				8.296	2	1825	0.124			
4.920	...	61	...				8.337	2	734	0.050			
4.974	1	768	0.048	1	1.40	0.130	8.377	2	2875	0.192			
4.984	1	726	0.046				8.417	2	2055	0.136			
5.037	1	152	0.009				8.469	2	1051	0.076			
5.159	0	~5400	~0.15	0	4.13	0.175	8.512	2	690	0.046			
5.219	2	1057	0.140	2	0.830	0.160	8.536	...	944	...			
5.389	2	786	0.099				8.578	2	2510	0.160			
5.425	4	431	0.816				8.649	2	1092	0.069			
5.461	2	2480	0.310	2	2.61	0.478	8.684	2	551	0.035			
5.505	(1)						8.713	2	632	0.039			
5.534	(1)	750	0.040				8.728	(2)	910	0.056			
5.570	0	6670	0.126	0	2.34	0.094	8.768	2	664	0.041			
5.620	1	724	0.040				8.808	2	1127	0.069			
5.692	0	13 900	0.268	0	4.66	0.183	8.839	2	703	0.043			
5.774	1	1135	0.061				8.855	2	861	0.052			
5.807	(2)	256	0.029				8.871	(2)	1200	0.072			
5.890	2	1340	0.164				8.895	2	1810	0.109			
5.940	...	~320	...	2	2.08	0.360	8.923	2	852	0.051			
5.978	1	909	0.047				8.950	(2)	1272	0.076			
6.049	...	352	...				8.984	...	~4000	...			
6.116	2	225	0.025				9.028	2	1625	0.095			
6.150	(1)	1000	0.050	...	0.70	...	9.062	(2)	902	0.052			
6.220	2	1060	0.112	2	0.613	0.100	9.113	2	1618	0.093			
6.249	2	495	0.052				9.167	...	~1700	...			
6.306	2	2035	0.292	2	1.87	0.302	9.206	(2)	694	0.072			
6.341	(2)	396	0.041				9.247	(2)	1390	0.077			
6.380	0	6760	0.175	(0)	3.72	.131	9.276	(2)	1050	0.058			
6.450	2	550	0.056	2	0.795	0.126	9.299	(2)	1755	0.097			

TABLE II. Results of the Ni<sup>60</sup>(*d,p*)Ni<sup>61</sup> reactions.

(1) Exci- tation energy (MeV)	(2)	This paper (3) $(\frac{d\sigma}{d\omega})_{\max}$ (Relative units)	(4) $(2J+1)S$	(5) <i>l</i>	Ref. 1 (6) $(\frac{d\sigma}{d\omega})_{\max}$ (mb/sr)	(7) $(2J+1)S$	(1) Exci- tation energy (MeV)	(2)	This paper (3) $(\frac{d\sigma}{d\omega})_{\max}$ (Relative units)	(4) $(2J+1)S$	(5) <i>l</i>	Ref. 1 (6) $(\frac{d\sigma}{d\omega})_{\max}$ (mb/sr)	(7) $(2J+1)S$
0	1	~7750	~1.67	1	9.50	1.58	5.372	(1)	86	0.007			
0.069	3	1175	3.37	3	1.91	3.52	5.413	2	486	0.081	2	1.26	0.197
0.290	1	~5950	~1.21	1	7.13	1.15	5.453	2	556	0.092			
0.654	1	214	0.040	1	0.173	0.026	5.537	2	465	0.076			
0.908	3	95.4	0.232	3	0.145	0.241	5.566	2	630	0.102	2	1.33	0.201
1.019	...	~9	...	...	...	...	5.608	2	401	0.064			
1.105	1	1058	0.183	1	0.880	0.125	5.647	2	622	0.098			
1.139	3	116	0.271	1	1.55	0.218	5.703	2	2410	0.375	2	6.58	0.98
1.195	1	1490	0.255	1	0.218	0.223	5.742	2	1720	0.265			
1.454	3	111	0.241	3	0.143	0.223	5.860	2	347	0.052			
1.622	...	~22	...	...	...	...	5.89	2	244	0.036			
1.750	1	176	0.027	1	0.228	0.028	5.95	2	118	0.017	0	2.15	0.067
2.133	1	~2060	~0.29	1	2.20	0.265	5.98	2	412	0.060			
	+	~1560	~7.1	+	1.98	6.2	6.00	0	1600	0.101			
	4			4			6.035	(2)	~90	~0.013			
2.473	(2)	19	0.006				6.073	2	244	0.035			
2.533	...	20	...				6.099	2	1440	0.205	(0)	1.73	0.052
2.633	1	471	0.062				6.168	...	~120				
2.694	2	~1820	~0.53	2	3.05	0.725	6.205	...	~300				
2.780	1	300	0.039	1	0.735	0.078	6.263	2	~550	0.077	2	2.06	0.27
2.800	3	90	0.148				6.320	2	410	0.056			
2.876	1	143	0.018				6.363	...	~300	~0.019			
2.905	2	40.5	0.011	0	0.180	0.009	6.389	(2)	630	0.085			
3.086	0	2960	0.083	0	1.54	0.077	6.40	2	360	0.048	2	1.15	0.15
3.127	(2)	140	~0.04				6.448	2	1420	0.189	2	2.08	0.27
3.305	(3)	~82	~0.02	3	0.253	0.281	6.479	2	236	0.312			
3.426	(2)	~100	~0.03				6.531	...	~300	...			
3.443	(2)	~100	~0.03				6.543	...	~300	...			
3.494	2	~4040	~1.0	2	5.00	1.04	6.609	...	300	...			
3.567	(2)	32	0.008				6.700	2	566	0.072			
3.649	2	774	0.186	2	1.13	0.236	6.727	...	~350	...			
3.679	1	414	0.045				6.800	2	834	0.102	(2)	1.06	0.14
3.709	...	130	...				6.892	(2)	625	0.076	0	1.53	0.042
3.743	0	2700	0.078	0	3.48	0.158	6.924	2	237	0.028			
3.877	2	194	0.045	2	0.78	0.153	6.97	...	1440	...			
3.923	...	121	...	3	0.602	0.628	7.019	...	900	...			
4.013	2	124	0.028				7.052	0	1090	0.108	0	3.94	0.106
4.088	...	46	...	3	0.133	0.137	7.099	2	267	0.031			
4.146	2	323	0.070	2	0.390	0.074	7.137	(2)	570	0.066			
4.200	...	120	...				7.185	(2)	200	0.022			
4.234	1	462	0.046	1	0.712	0.063	7.206	2	476	0.053			
4.318	...	510	...				7.232	2	620	0.074			
4.386	2	1240	0.255	2	1.32	0.245	7.276	...	~700	...			
4.472	2	1095	0.222	2	1.34	0.244	7.312	...	~600	...			
4.520	1	203	0.019				7.374	2	593	0.064			
4.560	0	96	0.004				7.437	2	569	0.060			
4.582	0	117	0.004				7.469	2	553	0.059			
4.727	1	94	0.008				7.509	2	464	0.049			
4.760	2	~2900	~0.55	2	4.71	0.79	7.557	2	561	0.059			
4.82	0	305	0.012				7.604	2	~650	~0.07			
4.877	2	392	0.072				7.620	2	~650	~0.07			
4.907	0	~6660	~0.25	0	5.36	0.206	7.698	2	710	0.071			
4.970	2	394	0.071				7.722	2	491	0.049			
5.070	0	4130	0.160	0	3.22	0.120	7.747	...	~300	...			
5.100	2	351	0.062				7.811	0	547	0.064			
5.134	1	705	0.059				7.826	2	213	0.021			
5.200	0	2750	0.115	0	1.72	0.115	7.865	2	630	0.060			
5.23	2	328	0.057				7.897	2	~340	0.03			
5.318	2	~920	~0.155	(0)	0.994	0.034	7.952	2	660	0.063			

for each isotope. The resulting spectroscopic factors are listed in column (4) of Tables I and II.

The last three columns of Tables I and II list the *l* values, absolute cross sections, and spectroscopic factors from Ref. 1. The agreement in *l* assignments between Ref. 1 and the present paper is very good. Where the few contradictory assignments occur, those of the present paper are considered more reliable because of better energy resolution and more complete angular distributions.

The spectroscopic factors of the present work tend to be relatively smaller than those of Ref. 1 for levels at high excitation energy. This effect can be explained by the improved energy resolution in the present data; this resolution distinguishes close-lying levels which would have been counted as a single proton group in the data of Ref. 1.

To obtain information on single-particle states from the data of Tables I and II, it is useful to assign spin values, *J*, to the nuclear levels. The (*d,p*) reactions can determine only values of *l*, not of *J*, but simple shell model considerations eliminate the ambiguity in spin assignments for *l*=0 (*s*<sub>1/2</sub>), *l*=3 (*f*<sub>5/2</sub>), and *l*=4 (*g*<sub>9/2</sub>). Ambiguities remain for *l*=1 (*p*<sub>3/2</sub> or *p*<sub>1/2</sub>) and *l*=2 (*d*<sub>5/2</sub> or *d*<sub>3/2</sub>). The spins of *p* levels were assigned as 1/2 except in cases where the spin is known<sup>8,9</sup> to be 3/2. This procedure gives results that are roughly consistent with sum rules on the intensities of *p*<sub>3/2</sub> and *p*<sub>1/2</sub> states.

Spins of the individual *d* levels were not assigned in

<sup>8</sup> *Nuclear Data Sheets*, edited by K. Way *et al.* (Printing and Publishing Office, National Academy of Sciences-National Research Council, Washington, D. C., 1962).

<sup>9</sup> G. A. Bartholomew and M. R. Gunye, *Bull. Am. Phys. Soc.* **8**, 367 (1963).

this study. The systematics of spin-orbit splittings of single-particle states indicate that most of the low-lying levels should be  $d_{5/2}$ , while most levels at high excitation energy should be  $d_{3/2}$ . But this evidence alone is not sufficient to assign spins to the many levels at intermediate excitation energies. Nevertheless, the location of the  $d_{5/2}$  and  $d_{3/2}$  single-particle states can be estimated from the data (see below, Sec. VI).

#### IV. COMPARISON WITH PAIRING THEORY

The sum  $\sum S(j)$  of the spectroscopic factors of all nuclear levels belonging to the shell-model state  $j$  is identical with the parameter  $U_j^2$  of pairing theory<sup>10</sup>; it is the normalized probability that the shell-model state  $j$  is completely empty. Values of  $\sum S$  are presented in column (2) of Table III and compared there with corresponding values from Ref. 1 in column (4), and from pairing theory in column (5). Column (3) of Table III lists values of  $\sum S$  from the present work whose magnitudes have been corrected for errors in magnitude of the DWBA parameter  $\sigma(l, \theta, Q)$  and in the experimental cross section. The correction consists of "normalizing" the absolute magnitudes of  $\sigma$  so that  $\sum S$  for all states observed on the  $\text{Fe}^{54}(d, p)\text{Fe}^{55}$  reactions are unity, as expected.<sup>11</sup> The necessary "normalization" factors have been obtained at an incident deuteron energy of 15 MeV and applied to the value of  $\sigma$  used in the present study. The  $s_{1/2}$ ,  $d_{5/2}$ , and  $d_{3/2}$  states have not been corrected; values of  $\sum S$  for these states, which are well above the ground state, should be unity if all levels have been observed.

Table III also presents the energies  $E_j$  of the single-particle states. The values of  $E_j$  are determined as the "centers of gravity" of the spectroscopic factors, or

$$E_j = \sum_i S_i(j) E_i / \sum_i S_i(j), \quad (2)$$

where the summation is over all nuclear levels belonging to the given shell model state  $j$ . The values of  $E_j$  from the present paper are listed in column (6) of Table III; they are compared with the results of Ref. 1 and pairing theory of columns (7) and (8), respectively.

The agreement between experimental and theoretical values of  $\sum S$  is quite good. This general agreement suggests specific conclusions about the two most serious cases of disagreement. Firstly, from the relatively small experimental value of  $\sum S$  for the  $s_{1/2}$  states in each isotope, we infer that not all the  $s_{1/2}$  levels have been observed. This conclusion agrees with the results of other data on the  $s_{1/2}$  levels (see below, Sec. VII). Secondly, the values of  $\sum S$  for the  $p_{3/2}$  and  $p_{1/2}$  states of  $\text{Ni}^{60}$  suggest that the ground state is not the only  $p_{3/2}$  level, as assumed above. The presence of  $p_{3/2}$  excited states with intensity sufficient to give the

TABLE III. Results for  $\text{Ni}^{58}$  and  $\text{Ni}^{60}$  and comparison with predictions of pairing theory.<sup>a</sup>

(1)	(2)	(3)	(4)	(5)	(6)	(7)	(8)
State	Present paper obs.	Present paper cor.	$\sum S$ Ref. 1	Pairing theory	Present paper	$E_j$ Ref. 1	Pairing theory
(A) $\text{Ni}^{58}(d, p)\text{Ni}^{59}$							
$p_{3/2}$	0.91	0.67	0.98 <sup>b</sup>	0.68	0.3	0.3 <sup>b</sup>	0
$f_{5/2}$	1.0	1.1	0.89	0.90	0.6	0.7	0.34
$p_{1/2}$	1.10	1.05	1.2 <sup>b</sup>	0.96	2.2	1.9 <sup>b</sup>	0.96
$g_{9/2}$	0.91	1.16	0.83	0.99	3.5	3.0	3.8
$d_{5/2}$	...	...	0.90	1.0	6.0 <sup>d</sup>	5.7	>4
$s_{1/2}$	0.53	...	0.41	1.0	7.3 <sup>c</sup>	5.8	>4
$d_{3/2}$	...	...	...	1.0	9.3 <sup>d</sup>	...	>4
(B) $\text{Ni}^{60}(d, p)\text{Ni}^{61}$							
$p_{3/2}$	0.41	0.31	0.40	0.43	0	0	0
$f_{5/2}$	0.72	0.79	0.84	0.76	0.4	0.9	0.01
$p_{1/2}$	1.18	1.12	0.98	0.90	1.2	0.9	0.43
$g_{9/2}$	0.71	0.91	0.62	0.99	2.1	2.1	3.1
$d_{5/2}$	...	...	0.95	1.0	5.0 <sup>d</sup>	4.6	>4
$s_{1/2}$	0.49	...	0.47	1.0	6.0 <sup>c</sup>	4.6	>4
$d_{3/2}$	...	...	...	1.0	8.4 <sup>d</sup>	...	>4

<sup>a</sup> Reference 10.

<sup>b</sup> These values use the spin assignments of Ref. 9.

<sup>c</sup> These results are discussed in Sec. VII of the text.

<sup>d</sup> These results are discussed in Sec. VI of the text.

predicted values of  $\sum S$  would increase  $E_j$  for the  $p_{3/2}$  single-particle state by about 0.3 MeV without significantly changing  $E_j$  for the  $p_{1/2}$  single-particle state.

The pairing-theory predictions of  $E_j$  which are listed in Table III have rather large uncertainties. Hence, there is reasonably good agreement between the experimental and theoretical values of  $E_j$ .

#### V. COMPARISON WITH GIANT RESONANCE THEORY

The giant resonance theory of Lane, Thomas, and Wigner<sup>12</sup> predicts that the width (full width at half-maximum) of the energy distribution of nuclear levels belonging to a single shell-model state should be approximately  $2W$ , where  $W$  is the imaginary part of the optical-model potential. It was shown in Ref. 1 that  $W$  may be related to the excitation energy  $E_j$  of shell-model states by

$$W \approx 0.33E_j. \quad (3)$$

The predictions of Eq. (3) are compared with the present experimental results in Fig. 3, which shows the various nuclear levels belonging to a single shell-model state as lines whose heights are proportional to the respective spectroscopic factors. The open circles in Fig. 3 mark the location of the "centers of gravity," while the horizontal lines indicate the width predicted by Eq. (3). In general, the agreement is quite good.

The "centers of gravity" shown for the  $s_{1/2}$  levels are taken from the results of a special study of those levels in Sec. VII. Likewise, the "centers of gravity" of the  $d_{5/2}$  and  $d_{3/2}$  states are taken from Sec. VI.

In  $\text{Ni}^{61}$  only one  $g_{9/2}$  level was observed, and in  $\text{Ni}^{59}$  only one strongly excited  $f_{5/2}$  level and one very weakly

<sup>10</sup> L. S. Kisslinger and R. A. Sorenson, Kgl. Danske Videnskab. Selskab, Mat. Fys. Medd. **32**, No. 9 (1960).

<sup>11</sup> R. H. Fulmer and A. L. McCarthy, Phys. Rev. **131**, 2133 (1963).

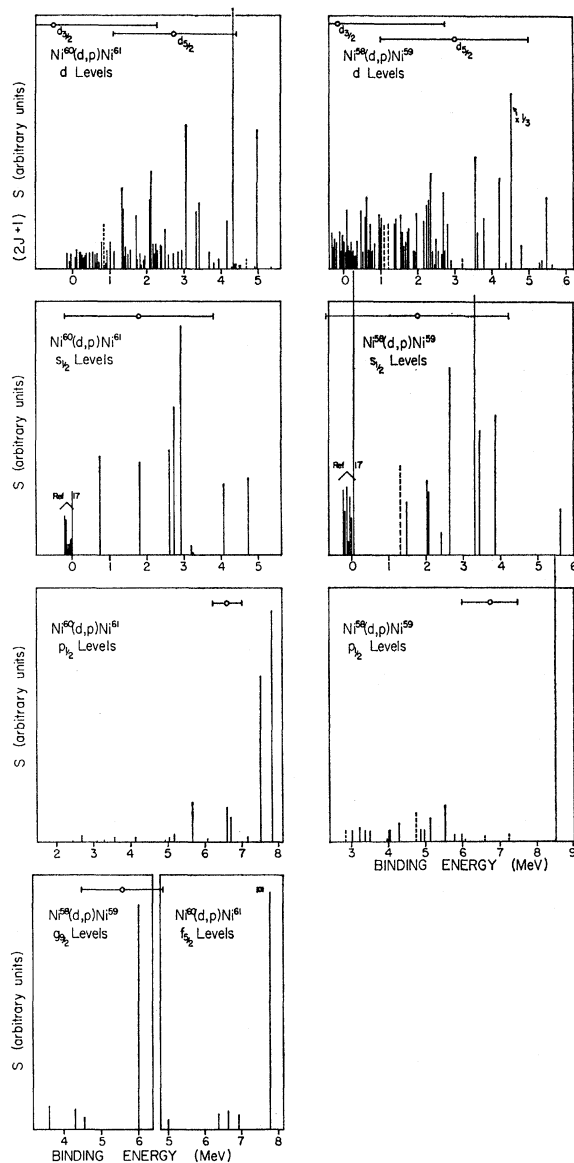


FIG. 3. Nuclear levels found in this work belonging to the shell-model states designated. Vertical lines represent position of levels, and their heights are proportional to the  $S$  values of Tables I and II; the latter are roughly proportional to cross sections. The dashed lines indicate uncertain  $l$  assignments. The open circles designate the "center of gravity" of these levels reported in Table III; the horizontal bars centered on the open circles designate the width of the single-particle levels expected from giant resonance theory. The "center of gravity" of the  $s_{1/2}$  nuclear level is determined not solely from the levels observed in this study; see Sec. VII of text. The determination of the "center of gravity" of the  $d$  levels is discussed in Sec. VI of text.

excited  $f_{5/2}$  level were observed. Figure 3 does not include these levels.

The facts that only one  $g_{9/2}$  level was observed in  $Ni^{61}$  and only one strongly excited  $g_{9/2}$  level was observed in  $Ni^{59}$  are somewhat inconsistent with the predictions of Eq. (3). Actually these effects are ex-

pected and can be explained by considering the configurations leading to  $9/2^+$  levels.

The configuration of any particle state in  $Ni^{59}$  and  $Ni^{61}$  can be expressed as the addition of a single particle to the configuration of a state in the respective target nucleus. Configurations leading to bound  $9/2^+$  levels in  $Ni^{59}$  and  $Ni^{61}$  are (1) the single-particle configuration, i.e. the ground-state configuration of the target plus a  $g_{9/2}$  particle, and (2) configurations formed by adding a  $p_{3/2}$  or  $f_{5/2}$  particle to the configuration of the lowest lying odd parity state of the target nucleus, namely the  $3^-$  state.

Configuration mixing will blend the single-particle configurations with the others, so that all  $9/2^+$  levels will have some single-particle components. The strength of this component in a particular level depends on the energy separation of the level from the original single-particle level however, and according to giant resonance theory<sup>12</sup> this energy separation must be less than  $W$  if the component is to be appreciable.

From Tables I and II and Eq. (3), appreciable mixing will occur for excitation energies less than about 4.1 MeV in  $Ni^{59}$  and 2.8 MeV in  $Ni^{61}$ . This energy limit in  $Ni^{59}$  is close enough to the energy of the  $3^-$  state of  $Ni^{58}$ , 4.5 MeV,<sup>13</sup> for a small amount of mixing to occur, and consequently a few weakly excited  $9/2^+$  levels should be observed in stripping reactions at about this excitation energy. The energy limit in  $Ni^{61}$  is much less than the energy of the  $3^-$  state of  $Ni^{60}$ , 4.1 MeV,<sup>13</sup> so that no mixing should be observed at all.

## VI. LOCATION OF $d_{5/2}$ AND $d_{3/2}$ STATES

As explained above, the spins of  $d$  levels cannot be determined in this investigation, and consequently the energy  $E_j$  of the single-particle  $d_{5/2}$  and  $d_{3/2}$  states cannot be obtained by simply applying Eq. (2). However, the locations of these states can still be estimated, using the following plausible assumptions:

- The ratio of intensities of the  $d_{5/2}$  to  $d_{3/2}$  levels is 6:4 because of the weighting factor of  $(2J+1)$  in the cross section.
- Because both states are completely empty,  $\sum S=1$  for each case.
- The principal nuclear energy levels belonging to the  $d_{5/2}$  state will almost all have smaller excitation energies than those belonging to the  $d_{3/2}$  state.
- From nuclear systematics,<sup>14</sup> the spin-orbit splitting of the  $d$  state is estimated to be about 3.3 MeV.

Estimations of the  $d_{5/2}$  and  $d_{3/2}$  energies, using different combinations of these arguments, are in agreement. The best energy estimates, in MeV, are for  $Ni^{59}$ ,

<sup>12</sup> A. M. Lane, R. G. Thomas, and E. P. Wigner, Phys. Rev. **98**, 693 (1955).

<sup>13</sup> R. K. Jolly, E. K. Lin, and B. L. Cohen, Phys. Rev. **128**, 2292 (1962).

<sup>14</sup> B. L. Cohen, Phys. Rev. **130**, 227 (1963).

$d_{5/2} \sim 6.0$ ,  $d_{3/2} \sim 9.3$ ; and for Ni<sup>61</sup>,  $d_{5/2} \sim 5.0$ ,  $d_{3/2} \sim 8.4$ .

The sensitivity of these results on the magnitude of the DWBA factor  $\sigma(l, \theta, Q)$  is such that the results are altered by about 0.3 MeV by a 10% change in  $\sigma$ . Considering possible errors from the uncertainty in  $\sigma$  and from reasonable experimental uncertainties, the final energy estimates for the  $d_{5/2}$  states are probably accurate to within about 1.5 MeV. The location of the  $d_{3/2}$  state is considered less certain because of the sensitivity of the result on both the reliability of assumption (d) above and on the reliability of the methods used.

#### VII. CORRELATION WITH NEUTRON DATA AND LOCATION OF $3s_{1/2}$ STATE

Since a  $(d, p)$  stripping reaction is essentially an insertion of a neutron into the nucleus, it is clear that there is a close relationship between the neutron width  $\Gamma_n$  and the stripping spectroscopic factor  $S$  for a given level. This relationship is expressed by formulas (4) to (10), which are valid for  $l=0$  neutrons. From Blatt and Weisskopf,<sup>15</sup>

$$\Gamma_n = 2kR\gamma^2, \quad (4)$$

where  $k$  is the neutron wave number,  $R$  is the interaction radius, and  $\gamma$  is the reduced width. The dimensionless reduced width  $\theta$  is

$$\theta = \gamma(\hbar^2/MR^2)^{-1/2}, \quad (5)$$

where  $M$  is the neutron mass. The spectroscopic factor  $S$  is then

$$S = \theta^2/\theta_0^2, \quad (6)$$

where  $\theta_0$  is the dimensionless single particle reduced width. Lane<sup>16</sup> has shown that to within about 30% uncertainty

$$\theta_0^2 \approx 0.6, \quad (7)$$

if we adopt

$$R = 1.45(A^{1/3} + 1) \times 10^{-13} \text{ cm}. \quad (8)$$

The neutron reduced width used in experimental papers,  $\Gamma_n^0$  is defined as

$$\Gamma_n^0 = \Gamma_n E^{-1/2} \text{ (eV)}. \quad (9)$$

From (4), (8), and (9), for Ni,

$$\gamma^2 = 316\Gamma_n^0$$

whence from (5), (6), and (7)

$$S \approx 7.0 \times 10^{-4} \Gamma_n^0. \quad (10)$$

From a comparison of Tables I and II with neutron total cross-section data,<sup>17</sup> we find two levels which have

TABLE IV. Results for levels studied by both neutron total cross sections<sup>17</sup> and  $(d, p)$  reactions.

Isotope	Neutron energy (keV)	Exc. En. ( $d, p$ ) (MeV)		$S$	
		Calc.	Obs.	Neutron	$(d, p)$
58	-28.5	9.005	8.984	0.05	0.10
60	14.5	7.825	7.811	0.015	0.032

been observed by both experiments; they are listed in Table IV.

The  $(d, p)$  levels of Table IV are identified with the neutron  $s_{1/2}$  resonance levels of Ref. 17 partially on the basis of energies; these levels occur at excitation energies which agree well within the experimental error with those calculated from the known neutron energies and  $Q$  values. Furthermore, the second level of Table IV is identified in this study as having  $l=0$ , and the first level of Table IV, while it cannot be assigned an  $l$  value because of experimental difficulties, nevertheless has an angular distribution consistent with an  $l=0$  assignment. For both the cases of Table IV, there are no other strong  $l=0$  levels near this energy in either the neutron or the stripping data, and so there is little chance for confusion. Finally, if the identifications are correct, the neutron data predict the existence at higher excitation energies of two  $l=0$  levels having intensity sufficient to be observed in the present stripping reactions. While these levels occur near the upper limit of experimental observability so that no definite angular momentum assignments are possible in this study, in each of the cases, levels are observed which are consistent in energy, intensity, and angular distribution with the levels predicted. We take this fact as further support for the correct identification of the levels of Table IV.

The last two columns of Table IV give the  $S$  values as obtained from the neutron data by use of Eq. (10), and from the stripping data (Tables I and II above). There is a factor of two discrepancy between the two determinations, but this is not unexpected. The neutron results are uncertain by perhaps 50% due to the uncertainty of the factor in Eq. (7) which was determined from data in a lighter mass region and even there with 30% uncertainty. The stripping results are uncertain by at least 50% both because of the unreliability of the DWBA calculations at this energy, and because the experimental measurements in this region are plagued by marginal energy resolution and high background. In view of these problems, we adopt the average of the two values as the best determination of  $S$ , and assign an error large enough to embrace both values. Thus Eq. (10) becomes

$$S \approx 1.0 \times 10^{-3} \Gamma_n^0 [\times (1.5)^{\pm 1}]. \quad (10')$$

The neutron strength function,  $\phi$ , is defined as

$$\phi = \sum \Gamma_n^0 / \Delta E, \quad (11)$$

<sup>15</sup> J. M. Blatt and V. F. Weisskopf, *Theoretical Nuclear Physics* (John Wiley & Sons, Inc., New York, 1952).

<sup>16</sup> A. M. Lane, *Rev. Mod. Phys.* **32**, 519 (1960).

<sup>17</sup> E. G. Bilpuch, K. K. Seth, C. D. Bowman, R. H. Tabony, R. C. Smith, and H. W. Newson, *Ann. Phys. (N.Y.)* **14**, 387 (1961).

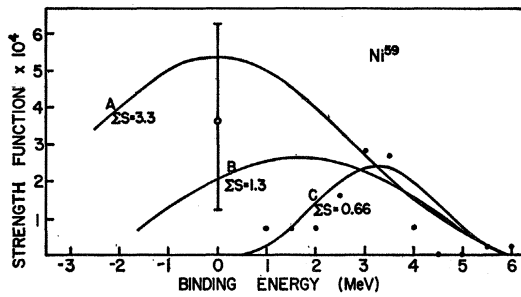


FIG. 4. Strength function of  $3s_{1/2}$  levels in  $Ni^{59}$ . The solid points are strength functions calculated from the data of the present work for an energy spacing of 1 MeV; the open circle is the strength function obtained from neutron resonance reactions (Ref. 17). The uncertainty shown on the latter point combines the error in its original determination with the uncertainty in its correlation with stripping data. Of the curves A, B, and C drawn through the experimental points, only B satisfies reasonable restrictions on the width of the curve and its area, which is shown in terms of  $\Sigma S$ .

where the numerator is the sum of  $\Gamma_n^0$  for all levels in a large energy interval,  $\Delta E$ . From Eq. (10'), this becomes

$$\phi = 1000 \Sigma S / \Delta E. \quad (12)$$

By use of (12),  $\phi$  can be calculated from the data of Tables I and II. Plots of  $\phi$  calculated with  $\Delta E = 1$  MeV are shown in Figs. 4 and 5. Also plotted are the  $\phi$  determined from neutron cross section data at zero neutron binding energy.<sup>17</sup> The errors shown on the points from the neutron data combine the errors from their original determination and the uncertainty of the factor in Eq. (10'). It is immediately clear from Figs.

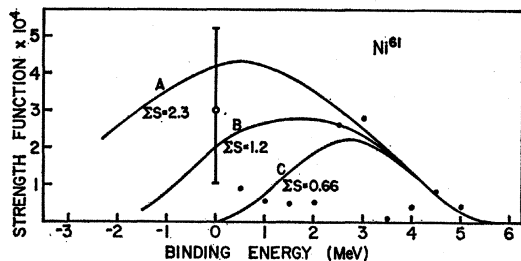


FIG. 5. Strength function of  $3s_{1/2}$  levels in  $Ni^{61}$ . See caption for Fig. 4.

4 and 5 that the data of Tables I and II miss very many  $l=0$  levels in the region of 0–2.5-MeV binding energy. This was also the conclusion from the results of Table III (Sec. IV). It is quite understandable in view of the facts that the energy resolution is rather marginal here, and the difference between DWBA angular distributions for  $l=0$  and  $l=2$  in this energy region is not large. For these reasons a given proton group could contain almost equal components of  $l=0$  and  $l=2$  and still be assigned simply as  $l=2$ .

A curve of  $\phi$  versus energy is expected to have two quantitative restrictions:

(1) Multiplying both sides of Eq. (12) by  $\Delta E$  and integrating over all energies,

$$\Sigma S = \frac{1}{1000} \int \phi \Delta E = 1, \quad (13)$$

where the last arises from the fact that  $\Sigma S = 1$  for a completely empty shell. Hence Eq. (13) gives a restriction on the area under the curve. In view of the uncertainties in the DWBA calculations, the expected area under the curve may deviate from Eq. (13) by as much as 50%.

(2) The width of the curve should be about  $2W$ , which, from Eq. (3) and Fig. 3 is about 5 MeV.

Two curves satisfying the second of these restrictions are passed through the data in Figs. 4 and 5. The lower of these (curve B), which in each case is practically the lowest that can fit the point from the neutron strength function, satisfies restriction (1) (above) within the expected error, whereas the upper curve (curve A) violates restriction (1) by a large factor. In both cases a third curve (curve C), which is drawn only through the points from the stripping data, also satisfies restriction (1), but the curve violates restriction (2) besides ignoring the data point from the neutron strength function. Thus the true curves must be something like the curves B. From this conclusion we see that the binding energy of the  $3s_{1/2}$  single-particle state is about 1.7 MeV in  $Ni^{59}$  and about 1.8 MeV in  $Ni^{61}$ . These estimates, which are listed in Table III, column (6), should be accurate to about 1 MeV. It thus seems that the neutron giant resonance occurs at a mass considerably lower than  $A = 58$ .